Fatigue crack initiation and early crack propagation in ultrafine-grained copper in high-cycle fatigue region

L. Kunz[1], P. Lukáš and L. Navrátilová

[1] Institute of Physics of Materials, Academy of Sciences of the Czech Republic, Žižkova 22, 616 62 Brno, Czech Republic

ABSTRACT. *Fatigue crack initiation and early crack propagation in ultrafine-grained copper prepared by equal channel angular pressing was experimentally investigated in high-cycle and giga-cycle region. The results of the observations are compared with those known for conventionally grained material. Dissimilarities and peculiarities of behaviour of ultrafine-grained structure are discussed.*
The cyclic slip localization in ultrafine-grained copper takes place in cyclic slip bands. The mechanism consists in highly localized slip within the individual ultrafine-grains resulting in development of cavities and voids arranged along the planes of highest cyclic shear stress and in formation of extrusions. The mechanism of the crack initiation in high- and giga-cycle fatigue region does not require grain coarsening often discussed in literature. Fatigue cracks initiate in long slip bands, which grow predominantly in zones of near-by oriented grains by subsequent linking of individual slip bands. A process of growth and linking of cavities and voids produced by the irreversible cyclic slip by dislocation movement generating point defects governs the early stage of the development of fatigue cracks. Sufficiently long cracks created by this mechanism and lying in suitably oriented long slip bands finally transform to fatigue cracks propagating by common opening mode with a plastic zone generated at their tip.

INTRODUCTION

Mechanisms of fatigue crack initiation and subsequent crack propagation has been a matter of intensive research in the past. For conventionally grained (CG) materials the comprehensive survey of basic knowledge on crack initiation, early crack propagation and propagation of long cracks can be found in many textbooks, e.g. [1, 2]. The particular and specific problems of crack initiation and propagation in advanced materials and in engineering structures are steadily a matter of research and discussion in scientific papers and contributions on specialized conferences, e.g. [3].

Ultrafine-grained (UFG) materials represent a group of advanced materials, having the grain size in the range of 100 to 1000 μm [4, 5]. They possess substantially better tensile properties when compared to CG metals and alloys. They are often prepared by severe plastic deformation, which enables to produce them in bulk. The reason of improved mechanical properties lies in the higher grain boundary volume in fine-

grained structures. This makes the dislocation motion and resulting plastic deformation more difficult. For many materials the yield stress follows the Hall-Petch equation in a very broad range of grain size between 1 μm and 1 mm [6]. The grain size of UFG materials is below 1 μm and above that of nano-grained structures having the grain size below 100 nm. Thus UFG materials represent a transition from CG structures to nano-grained ones; this transition is related to their peculiar properties.

Historically, the great deal of the pool of basic knowledge on fatigue damage mechanisms, development of dislocation structures, cyclic plastic strain localization, crack initiation and its relation to microstructure have been conducted on f.c.c. materials, particularly on Cu. The same holds for the pioneering investigation of fatigue performance of UFG material processed by severe plastic deformation [7, 8]. Cu belongs from this point of view to the most thoroughly investigated materials. This is also the reason why it was chosen for investigation in this study.

The simple general rule indicates that the value of fatigue or endurance limit for most CG steels and copper alloys is 35 to 50 % of the ultimate tensile strength σ_{UTS} [2]. This signalizes promising fatigue resistance of UFG materials and makes them attractive for engineering applications. Indeed, the fatigue lives of UFG specimens were generally found to be larger than those of CG specimens when fatigue tests were conducted under stress control and expressed in terms of S-N plots [9]. UFG Cu prepared by equal channel angular pressing (ECAP) with σ_{UTS} = 387 MPa exhibits under stress-controlled fatigue loading endurance limit of 150 MPa (on the basis of 10^8 cycles) [10]. However, the rule, relating the fatigue limit to the σ_{UTS} is sometimes violated in UFG materials. For instance, for the UFG Cu having σ_{UTS} 390 or 420 MPa (in dependence on the details of the UFG structure), the experimentally determined endurance limit was only 80 MPa, which is very close to the value characteristic for an annealed CG copper [11]. These substantially unmatched results were recently discussed, e.g. in [9, 10]. The explanation is currently sought in the stability of the UFG structure under fatigue loading and, consequently, in the details of the fatigue crack initiation and early crack propagation. Nonetheless, the up-to now available knowledge is not sufficient to explain the observed effects consistently.

Fatigue of CG easy cross-slip materials, like Cu and Al under constant stress amplitude loading depends only very weakly on the grain size [12]. A weak decrease of the endurance limit (based on 10^9 cycles) expressed in terms of the total strain amplitude with increasing grain size was reported in [13]. Generally, it can be summarized that the fatigue life curves expressed both as S-N curves or dependences of number of cycles to failure on the total strain amplitude depend on the grain size insignificantly. This holds especially for endurance limits defined for 10^7 cycles [12]. Based on results published e.g. in [12-14] it can be concluded, that the fatigue strength of Cu in high-cycle region is nearly insensitive to the grain size ranging from 3 to 1200 μm. The explanation of this insensitivity to the grain size utilizes the idea, that the dislocation cell structure, which develops in CG materials due to fatigue, masks the effect of the grain size [12]. UFG materials prepared by ECAP also exhibit a cell structure. However, it differs in details from that developed in Cu under fatigue loading. The UFG material reveals substructural features - subgrains, dislocation cells and X-ray

coherent diffraction regions. The structure bears traces of the ECAP process. The cells are often elongated in the shear direction along the last ECAP plane. The details of the structure are dependent on the ECAP route; the Bc route yields the structure of highest equiaxiality. Further, the scatter of the cell size is often substantial. Quantitative determination of grain or cell size of materials processed by ECAP is complicated by the fact that the size is varying broadly between hundreds of nanometers and some microns and by not well-defined boundaries in TEM images. The mutual orientation of structural units cannot be satisfactorily described as homogeneous high-angle random orientation. That is why the term grain size is often replaced by the term cell size to point out that there are areas containing crystallites with very similar orientation. There are regions where the low angle boundaries are frequent. These regions can be described as "zones of near-by oriented grains" and they seem to play an important role in the localization of cyclic plasticity, crack initiation and early crack propagation [15].

The fatigue strength of cyclically loaded Cu is determined by cyclic slip localization, initiation of fatigue cracks and early crack propagation. The complete solution of the damage by fatigue needs together with the knowledge on cyclic slip localization mechanism primarily the knowledge on the crack initiation process, including the crack path in the early fatigue crack stage. The mechanism of crack initiation known from CG materials cannot be directly applied to UFG structures. In the CG Cu the crack initiation and early crack propagation is related to the persistent slip bands (PSB). Important role plays the surface roughness (extrusions and intrusions), which develops during cycling on the free surface. The characteristic dimension of specific dislocation structure below the surface relief, i.e. the width and length of the ladder-like PSB structure in the case of low-amplitude loading or the dimension of layers of dislocation cells in the case of high-amplitude loading, substantially exceeds the characteristic structural dimension of UFC Cu. Here, contrary to the case of CG Cu or Cu single crystals, where the characteristic dislocation structures develop, no specific dislocation structures were detected [9].

Summarizing the up-to now state of art, there is no satisfactory explanation and understanding of the cyclic slip localization, crack initiation and early crack propagation in UFG Cu at present. Simultaneously, it is obvious that the knowledge obtained on CG copper cannot be directly utilized for UFG structure. The aim of this study is to investigate the initiation and early crack propagation in UFG Cu and to contribute to the completion of the knowledge on this phenomenon.

ULTRAFINE-GRAINED COPPER

Copper of 99.9% purity was processed by ECAP. Cylindrical billets of 20 mm in diameter and 120 mm in length were produced by eight passes through the die using the route Bc (90° rotation after each extrusion). The ECAP procedure was carried out at room temperature. After the last ECAP path samples of 16 mm in diameter and 100 mm length were turned from the billets. The billets were marked after the last ECAP path in such a way that identification of the two main longitudinal axial planes, namely the

plain “1” and plane “2” (perpendicular to the plane”1”) was possible on the finished specimens, Fig. 1. The transversal plane is marked as “3”. The reason was to enable the correlation of the observed structures after fatigue with the orientation of the shear plane, which was active in the last ECAP paths.

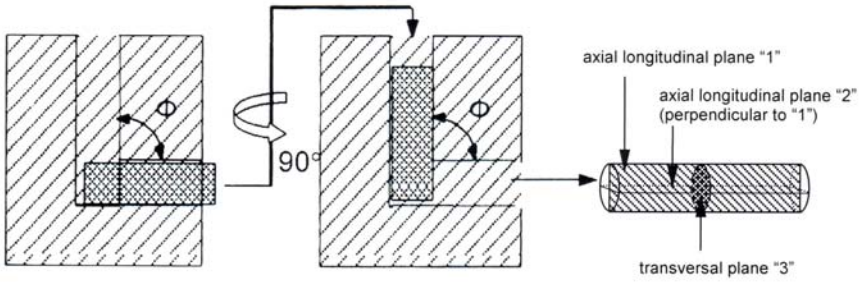

Figure 1. Scheme of ECAP and identification of the axial longitudinal and transversal planes in the billet after last pass through the die.

Figure 2. Microstructure on axial longitudinal section by plane “1”, LM.

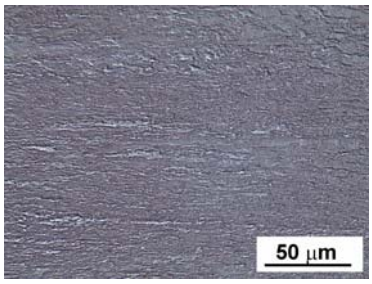

Figure 3. Microstructure on axial longitudinal section by plane “2”, LM.

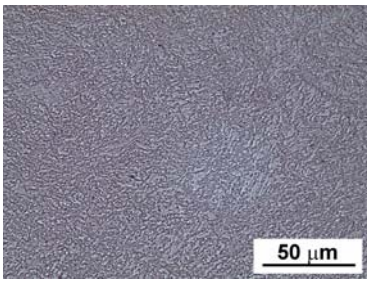

Figure 4. Microstructure on transversal section by plane “3”, LM.

Tensile properties of UFG Cu were determined by means of a standard tension test on 4 cylindrical specimens of 5 mm in diameter on a Zwick tensile machine. The specimens were turned from the billets and their surface was finished by fine grinding. The ultimate tensile strength was 387 ± 5 MPa, the yield stress $\sigma_{0.1} = 349 \pm 4$ MPa, $\sigma_{0.2} = 375 \pm 4$ MPa and the modulus of elasticity $E = 115 \pm 11$ GPa.

The microstructure as observed by means of light microscopy (LM) on polished and etched ($K_2Cr_2O_7 + H_2SO_4 + H_2O$) sections is shown in Figs. 2, 3 and 4. The structure as observed on a section by the plane “1” exhibits directionality, Fig. 2. Some degree of directionality was found also on the section by the plane “2”, Fig. 3. The structure on the transversal section, Fig. 4, was most homogeneous, without traces of directionality.

The microstructure as observed by transmission electron microscopy (TEM) in the middle of the cylindrical sample is shown in Figs. 5 and 6. The dislocation structure characteristic for the axial longitudinal section can be seen in Fig. 5. Similarly to the observation by LM, Fig. 3, some directionality expressed by elongated cells was observed on some foils. However, there are regions, where the cell structure is equiaxial and similar to that in the transversal section. The dislocation structure typical for the transversal section is shown in Fig. 6. The average grain (cell) size, determined on 10

electron micrographs, both from longitudinal and transversal sections is 300 nm. This is in agreement with other investigations, e.g. [8, 16, 17].

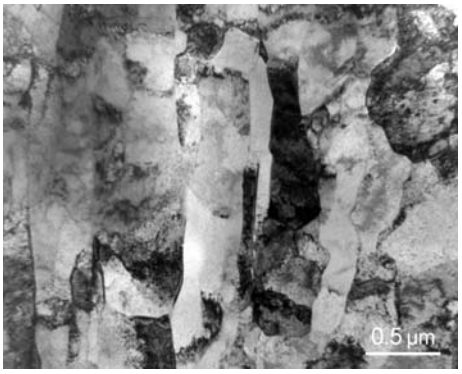

Figure 5. Microstructure on axial longitudinal section by plane "1", TEM.

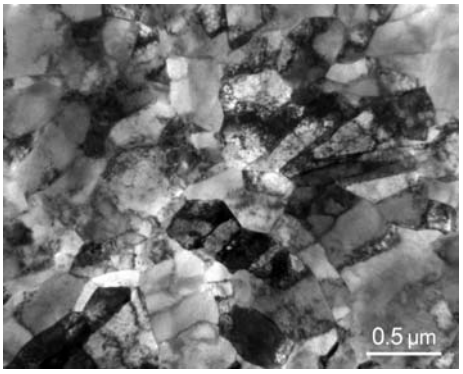

Figure 6. Microstructure on transversal section by plane "3", TEM.

EXPERIMENTS

Fatigue tests were carried out on cylindrical specimens, turned from ECAPed billets. Tests were conducted under controlled load in symmetrical push-pull cycling, i.e. with the stress ratio R = -1. Two testing systems were used.

A servohydraulic testing machine was applied for tests with the number of cycles to failure not exceeding 7 x10^6 cycles. The diameter of the gauge section of specimens was 6 mm. The frequency of cycling was of about 10 Hz.

An ultrasonic testing system operating at frequency of 20 kHz was used for the very long-life tests with the number of cycles to failure of the order of 10^{10}. For these tests specimens with a minimum diameter 4 mm were used. The specimens were cooled by current of air to keep the temperature of the gauge length during the test below 50 °C.

Observation of the surface of fatigued specimens was carried out by means of scanning electron microscope (SEM) Tescan Lyra 3XMU® equipped with focused ion beam (FIB). The gauge length of the specimens was fine polished after turning. Just before the fatigue testing the gauge length was carefully electrolytically polished. FIB technique was used for observation of the slip bands relief. Ion-channelling contrast in scanning ion microscopy (SIM) was applied for visualization of subsurface microstructure.

RESULTS

Fatigue loading results in cyclic slip localization, which manifests itself on the specimen surface by development of surface slip bands. An example of surface relief developed on an electrolytically polished specimen after fatigue loading with controlled stress amplitude σ_a = 170 MPa is shown in Fig. 7. The slip localization is very pronounced. Typically, groups of parallel slip bands appear on the surface which otherwise does not

exhibit any traces of slip activity. The bands in Fig. 7 correspond to the number of cycles 6.2 x 10^6. The longitudinal lengths of some bands exceed substantially the grain size of the UFG Cu, which is 300 nm. Extrusions with variable height with intrusions along them develop.

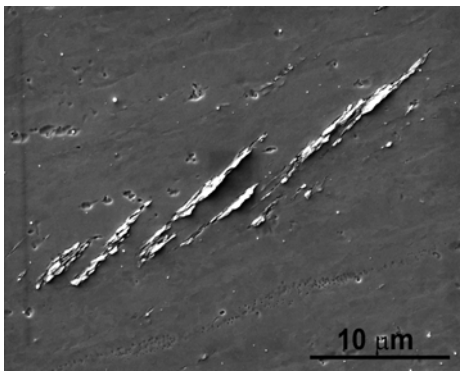

Figure 7. Cyclic slip bands developed after fatigue loading with σ_a = 170 MPa. Number of cycles 6.2 x 10^6.

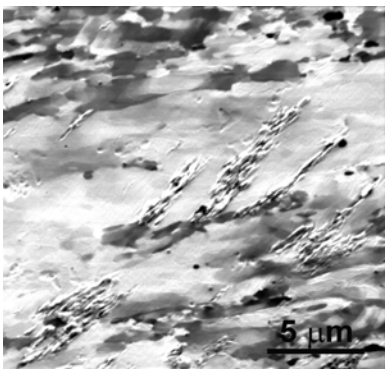

Figure 8. Cyclic slip bands in a zone of near-by oriented grains. σ_a = 130 MPa. Number of cycles 2.3 x 10^{10}.

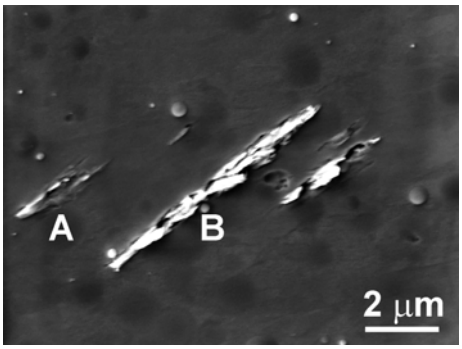

Figure 9. Cyclic slip band, σ_a = 170 MPa. Number of cycles 9.5 x 10^5.

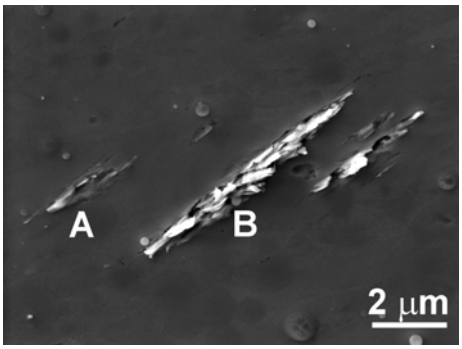

Figure 10. Cyclic slip band, σ_a = 170 MPa. Number of cycles 6.2 x 10^6.

Figure 8 shows the slip bands as observed by means of SEM using ion-channelling contrast. This mode of visualization enables to observe simultaneously the surface relief together with the grain structure. The individual differently oriented grains are displayed by different shade of grey. The higher is the disorientation between the neighbouring grains the higher is the contrast. It is obvious from Fig. 8 that the cyclic slip bands grew up in the zone where the grey contrast of neighbouring grains is low, which indicates that the disorientation between the grains is small. This zone can be called "zone of near-by oriented grains" [18]. Outside this zone the neighbouring grains obviously have higher mutual disorientations.

The slip bands do not develop continuously during the whole fatigue life. The band A shown in Fig. 9 corresponds to the number of cycles 9.5 x 10^5 at σ_a = 170 MPa. The next fatigue loading up to the 6.2 x 10^6 cycles did not change the slip band appearance detectably, Fig. 10. It means that the initial irreversible slip activity in this region was

exhausted. The band B changed its appearance between 9.5 x 10^5 and 6.2 x 10^6 only moderately. Its length extended slightly, whereas the width of the band somewhat extended and the number of extrusions and their height slightly increased.

The slip bands on the surface of the specimen loaded at the stress amplitude σ_a = 170 MPa can be found on the whole circumference of the fatigue specimen gauge length. The majority of them make an angle in the range from 30 to 60 degrees to the direction of the cyclic loading. For instance, in the case of bands shown in Figs. 7-14 the stress axis was horizontal. Sporadically were observed also short and thick slip bands, Fig. 11, inclined at a high angle to the loading direction. Such bands were found mainly in regions near to the intersection of the specimen surface with the plane "1".

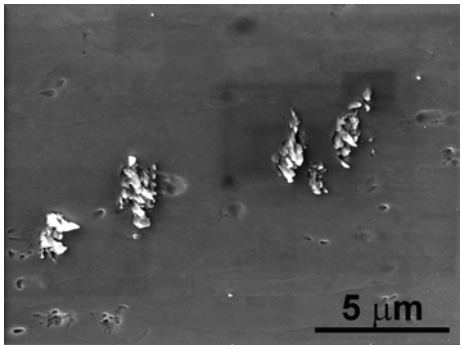

Figure 11. Slip bands inclined at a high angle to the loading axis.

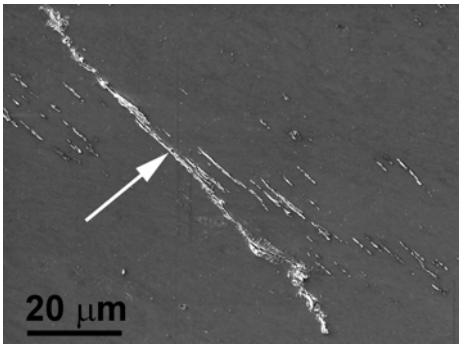

Figure 12. Fatigue crack. Number of cycles 6.2 x 10^6.

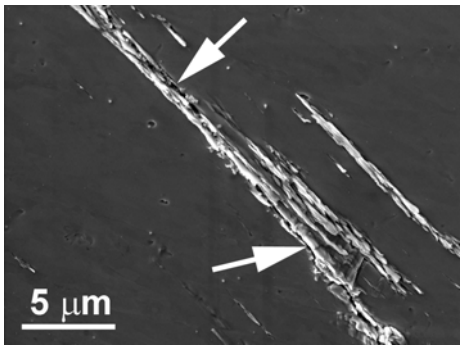

Figure 13. Central part of fatigue crack.

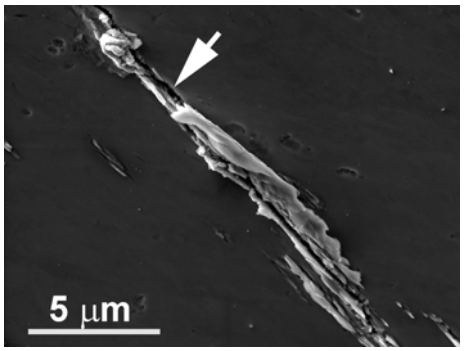

Figure 14. Central part of fatigue crack.

Fatigue cracks initiate in cyclic slip bands. The arrow in Fig. 12 indicates such a fatigue crack. It appeared in a group of bands lying in a zone of near-by oriented grains. The crack is narrow in its central region and evidently spreads from a long slip band. The central part of the crack is shown in Fig. 13 at higher magnification. White arrows indicate the crack situated lengthwise the extrusions. They are high and hide the crack "mouth" on the surface on many places. Nevertheless, the careful observation results in a conclusion that the crack is continuous and runs along the whole long slip band. In the vicinity of the crack, in its central region, no secondary slip activity induced by the existing crack is apparent, Fig. 14. The arrow indicates a fracture

surface, where the material does not exhibit any visible traces of an irreversible slip activity in the closest vicinity of the crack.

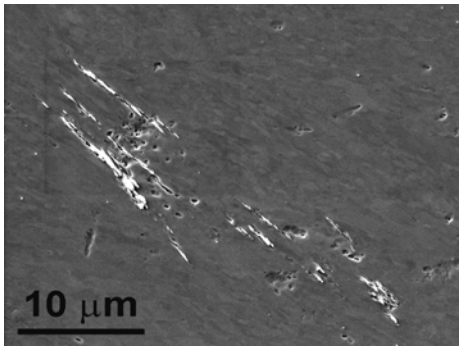

Figure 15. Slip bands after 9.5 x 10^5 cycles.

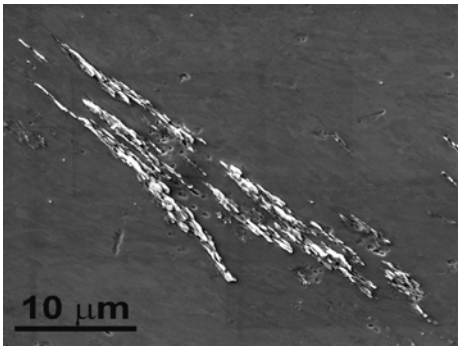

Figure 16. The same area as in Fig. 15 after 6.2 x 10^6 cycles.

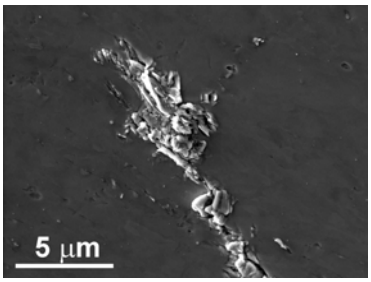

Figure 17. Tip of the fatigue crack shown in Fig. 12 (left upper corner).

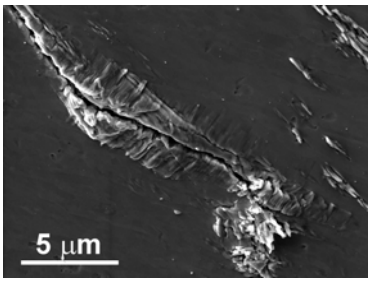

Figure 18. Tip of the fatigue crack shown in Fig. 12 (right bottom corner).

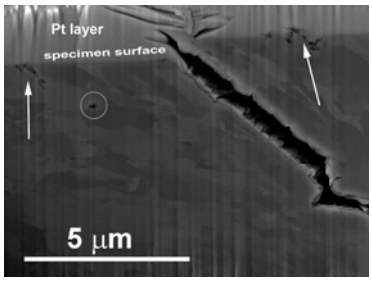

Figure 19. Section through fatigue crack in its central part.

The fatigue cracks develop from long slip bands. Evolution of long bans during high-cycle fatigue is documented in Figs. 15 and 16. The first one shows a region with slip bands, which were formed during the first 9.5 x 10^5 cycles. The second Figure displays the same area after 6.2 x 10^6 cycles. The length and the width of the slip bands have increased. However, new bands appeared in areas, which were free of bands after 9.5 x 10^5 cycles, Fig. 15. There is a tendency for development of slip bands tilted at the same angle to the loading axis and concatenating along one line. Successive development of new bands and a moderate growth of old ones in length finally results in creation of long slip bands. Indeed, the condition of near-by oriented zone of grains in this region has to be fulfilled.

Fig. 12 indicates that the fatigue crack on both ends exhibits fuzzy crack paths, contrary to its middle part. Both the crack tips are displayed in detail in Figs. 17 and 18. Secondary slip bands are visible in the crack wake and near the crack tips. The slip bands in the right upper corner in Fig. 18 were produced by the fatigue loading of the bulk material; the slip bands near the crack tip are a result of the cyclic stress concentration at the tip of the propagating crack.

FIB technique has been used to visualize the sections perpendicular to the fatigue crack. A platinum protective layer was applied transversally on the crack in its central part by beam-induced deposition. The region was subsequently FIB milled. Fig. 19 shows a micrograph of a cut perpendicular to specimen surface. Evidently opened fatigue crack inclined to the specimen surface nearly at an angle of 45 degrees can be seen. The distance between the matching fracture surfaces is of about 1 μm. The ion-channelling contrast in SIM enables to visualize the microstructure round the crack. The crack direction seems to reflect the structural directionality. The crack path is straight near the specimen surface and apparently transgranular. Arrows in the Figure indicate slip bands on the surface and related subsurface damage. In some places below the surface cavities or voids can be found; an example of an isolated one is encircled.

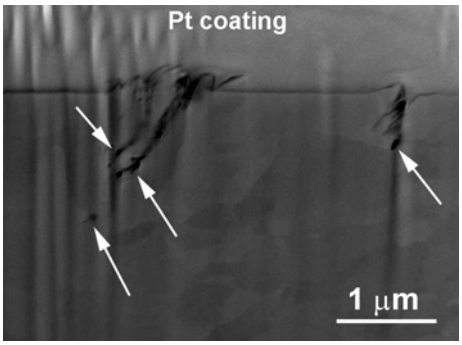

Figure 20. FIB micrograph of a cut through cyclic slip bands and grain structure.

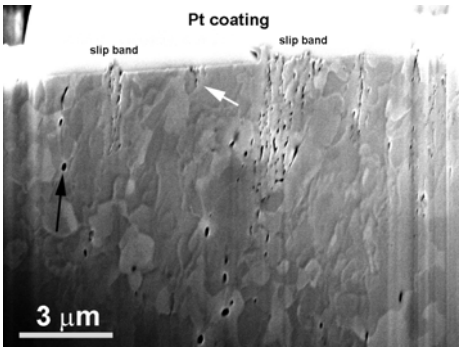

Figure 21. FIB micrograph showing a cut through cyclic slip bands and grain structure after giga-cycle fatigue.

FIB section through two slip bands on the surface of a specimen after loading with $\sigma_a = 170$ MPa for 6.2×10^6 cycles is shown in Fig. 20. The damage consists of extrusions protruding from the surface to the height up to 0.5 μm. The damage in material interior, below the surface relief consists of voids, indicated by arrows in the Figure. The voids are interconnected with areas of damaged material exhibiting clear discontinuity. The damage tends to be located along the planes, which apparently have the best conditions for the cyclic slip. The ion-channelling image of structure shows that the damage related to the larger slip band is situated across one surface grain and proceeds to a void on the grain boundary.

Similar development of damage was observed also after giga-cycle fatigue. The frequency of slip band occurrence on the surface of specimens is substantially lower that after high-cycle fatigue. FIB section through slip bands on the surface of a specimen after loading with 2.4×10^{10} cycles at ultrasonic frequency is shown in Fig. 21. Broad slip bands with extrusions rising again up to 0.5 μm above the surface are clearly visible. The appearance and size of the grains beneath the surface relief do not differ from those in other places. No grain coarsening can be observed. The fatigue damage in material interior consists of cavities, often elongated and arranged in rows. In

material interior numerous isolated cavities or voids were formed. They are located not only on the grain boundaries, but also within the grains.

DISCUSSION

The fatigue damage mechanism of UFG Cu exhibits differences to that known from CG material due to very small grain size. In CG Cu at low stress amplitudes, i.e. in high-cycle fatigue region, most of the grains which show slip bands have only one slip system active. The slip bands are long and terminate at the grain boundaries or free surface. Their dimension is governed by the grain size and orientation varies grain to grain. Usually small grains do not exhibit any slip. This is explained by elastic compatibility of adjacent large grains. Smaller grains have stronger constraints and, therefore, have a more complex stress state with the same maximum stress [19]. The slip bands in UFG Cu are substantially shorter than in CG Cu. Their activity during fatigue loading often ceases. The mechanism of formation of long slip bands, which later on transform into fatigue cracks, consists in development of groups of slip bands, which are on the specimen surface inclined at nearly the same angle to the loading axis, see Fig. 12, and subsequent formation, growth and concatenating of individual bands.

An important phenomenon is initiation and growth of new slip bands in course of fatigue process in regions, which did not exhibit any substantial activity at the beginning of loading. In zones of near-by oriented grains, which can be identified by ion-channelling contrast, long slip bands gradually develop. The cyclic plasticity, which manifests itself by the development of observable surface relief, is in this phase of fatigue damage restricted to the bands. No traces of fine slip or some damage of material surface (as observed in CG Cu) can be seen in the vicinity of the band. In sufficiently long bands surface observation by SEM reveals deep interconnected intrusions situated lengthwise the extrusions.

Based on the observation by ion-channelling contrast on the specimen surface and on FIB sections of the slip bands the optimal conditions for development of long slip bands are in zones of near-by oriented grains. From FIB sections, Figs. 19 - 21 it follows that the fatigue damage in the form of cavities (voids) develops within the individual surface grains, whose crystallographic orientation is suitable for cyclic slip. Arrows in Figs. 19 and 21 indicate such damaged grains. The cyclic slip activity is not restricted only to the surface grains. In material interior cavities (voids) are generated due to irreversible movement of dislocations. This is most pronounced under giga-cycle fatigue, Fig. 21. Point defects, generated by dislocation interactions have to play and important role in the mass transfer necessary for creation of voids. The UFG materials are characteristic by higher volume of grain boundaries when compared to CG ones. It can be anticipated that the grain boundary sliding plays an important role in accommodation of the constraints of neighbouring grains and can be driving force for dislocation activity within individual grains.

It is noteworthy to mention, that similar observation of surface relief and cracks inclined at an angle of 45 degrees to the surface were found after giga-cycle fatigue of CG Cu [20]. The authors consider the observed cracks as mode II stage I shear cracks.

The presented observations do not witness instability of UFG structure, which is often discussed in relation to the fatigue performance, e.g. [21-23]. The grain coarsening or formation of bi-modal structure was not observed. The stability of structure explains also the substantially higher fatigue performance in high- and giga-cycle region, observed under loading with constant stress amplitude [10].

Fatigue cracks develop from damage starting in particular grains. FIB sections indicate that the intrusions like those visible e.g. in Figs. 9, 10 correspond to cavities or voids reaching the surface in the slip band, Figs. 20, 21. The crack in high-cycle fatigue region forms by connecting of rows of these defects situated on and below the surface. The mechanism of the increase of the crack length on the surface consists in subsequent development of slip bands in the closest neighbourhood; the necessary condition is that the bands form a row oriented at suitable angle to the loading axis. The growth towards the materials interior is at the beginning realized by growth and coalescence of cavities (elongated voids). Natural condition for this mechanism is existence of near-by oriented regions of grains, which have suitable common orientation to the loading axis. Later on in the fatigue process the crack formed in this way starts to propagate by the common opening mode along the slip bands formed due to stress concentration at the crack tip. This mechanism of crack growth is in agreement with recent observations published by Goto et al. [24]. At the end of the crack a plastic zone in the fracture mechanical sense develops. The cyclic stress concentration produces secondary cyclic slip bands in this zone, which is clearly visible in Figs. 12, 17 and 18, showing the tips of a crack having the length of about 90 μm.

The cyclic slip with small amount of irreversibility takes place in the grain interior. This slip irreversibility together with the mass transfer by the point defects causes the growth of the surface relief; extrusions with the height up to 0.5 μm develop. The operation of slip on parallel slip planes within the grains, resembling the fine slip in CG Cu were observed in the plastic zone of the crack propagation by the common opening mode I, Fig. 17.

CONCLUSIONS

Fatigue cracks in UFG Cu loaded in high-cycle and giga-cycle region initiate in cyclic slip bands. The localization of cyclic plasticity is very pronounced and starts within the individual grains. Long slip bands develop in regions of near-by oriented grains. The fatigue damage in the slip bands consist in formation of cavities and elongated voids, which later on link along the planes with the highest cyclic shear stress. Grain boundary sliding plays an important role in accommodation of the constraints of neighbouring grains and can serve as driving force for dislocation activity within individual grains. The dynamic grain coarsening, often thought over in relation to fatigue damage of UFG Cu is not a prerequisite for crack initiation. Fatigue cracks initiate within the long slip bands and later on propagate by the common opening mode.

A plastic zone in fracture mechanical sense is generated at the crack tip due to cyclic stress concentration. The zone manifests itself by creation of secondary slip bands, which further predetermine the crack path on the microscopic level.

ACKNOWLEDGEMENT

The Czech Science Foundation under contract 108/10/2001 and the project "CEITEC - Central European Institute of Technology" CZ.1.05/1.1.00/02.0068 financed by European Regional Development Fund financially supported this work. The support is gratefully acknowledged.

REFERENCES

1. Klesnil, M., Lukáš, P. (1992) *Fatigue of Metallic Materials*, Academia/Elsevier Prague.
2. Suresh, S. (1998) *Fatigue of Materials*, Cambridge university press, Cambridge.
3. *The int. conference on "Crack Paths"*. Available on http://www.cp2012.unipr.it.
4. Valiev, R. Z., Islamgaliev, R. K., Alexandrov, I. V. (2000) *Progr. Mater. Sci.* **45** 103-189.
5. Zhu, Y.T., Langdon, T.G. (2004) **JOM,** October, 58-63.
6. Saada, G. (2005). *Mater. Sci. Eng. A*, **400-401**, 146-149.
7. Agnew, S. R., Weertman, J. R. (1998). *Mater. Sci. Eng. A*, **244**, 145-153.
8. Agnew, S. R., Vinogradov, A. Yu., Hashimoto, S. Weertman, J. R. (1999) *J. Electronic Mater.* **28**, 1038-1044.
9. Mughrabi, H. (2010) *Procedia Engineering* **2** 3-26.
10. Kunz, L., Lukáš, P., Svoboda, M. (2006) *Mater. Sci. Eng.* **A424**, 97-104.
11. Vinogradov A, Hashimoto, S. (2001) *Materials Transactions* **42**, 74-84.
12. Thompson, A., W., Backofen, W. A. (1971) *Acta Metallurgica* **19**, 597-606.
13. Müllner, H., Weiss, B., Stickler, R., Lukáš, P., Kunz, L. (1984) In: *Fatigue 84. Proc. of the 2nd Int. Conf. on Fatigue Thresholds,* Beevers, C. J. ed., Engineering Materials Advisory Services Ltd., 423-434.
14. Lukáš, P., Kunz, L. (1987) *Mater. Sci. Eng.* **85**, 67-75.
15. Kunz, L., Lukáš, P., Pantělejev, L. Man, O. (2011). *Procedia Engineering* **10**, 201-206.
16. Mingler, B., Karnthaler, H. P., Zehetbauer, M., Valiev, R. Z. (2001). *Mat. Sci. Eng. A*, **319-321**, 242-245.
17. Besterci, M., Kvačkaj, T., Kováč, L., Sűlleiová, K. (2006). *Kovove Mater.* **44**, 101-106.
18. Lukáš, P., Kunz, L, Navrátilová, L., Bokůvka, O. (2011) *Mater. Sci. Eng.* **A 528,** 7036-7040.
19. Wang, Z., Laird, C. (1988) Mater. Sci. Eng. **100** 5-68.
20. Weidner, A., Amberger, D., Pyczak, F., Schönbauer, B, Stanzl-Tschegg, S., Mughrabi, H. (2010) *Int. J. of Fat.* **32**, 872–878.
21. Kwan, Ch., C., F., Wang, Z. (2011). *Mat. Sci. Forum,* Vol. 683, 55-68.
22. Mughrabi, H., Höppel, H., W., (2001). In: *Mat. Res. Soc. Symp. Proc.* Farkas, D. et al. (Eds.), Mater. Res. Soc. Warrendale Penn. Vol. 634, p. B2.1.1-B2.1.12.
23. Mughrabi, H., Höppel, H., W., (2010). *Int. J. Fatigue*, Vol. **32**, 1413-1427.
24. Goto, M., Ando, Y., Han, S. Z., Kim, S. S., Kawagoishi, N., Euh, K. (2010), *Eng. Fract. Mech.* **77,** 1914–1925.